THE NATURE OF CHEMICAL BOND IN TRIOXIDE γ-UO_3

by

Yury A. TETERIN[1], Mikhail V. RYZHKOV[2], Anton Yu. TETERIN[1], Alexander D. PANOV[1], Anton S. NIKITIN[1], Kirill E. IVANOV[1], and Igor O. UTKIN[1]

Received on October 9, 2002; accepted on October 21, 2002

Low-energy X-ray photoelectron and conversion electron spectra from uranium trioxide were measured, and calculations were done for the $[UO_2O_4]^{6-}$ (D_{4h}) cluster which reflects the structure of uranium close environment in γ–UO_3 in the non-relativistic and relativistic X_α-DVM approximation. This enabled a satisfactory qualitative and in some cases quantitative agreement between the experimental and theoretical data, and interpretation of such spectra. Despite the traditional opinion that before participation in the chemical binding, the U5f electrons could be promoted to the higher (for example – U6d) levels, it was theoretically proved and experimentally confirmed that the U5f electrons (about two U5f electrons) are able to participate directly in the chemical bond formation in uranium trioxide. The filled U5f states proved to be localized in the outer valence molecular orbitals energy range 4–9 eV, while the vacant U5f states were generally localized in the low-energy range (0–6 eV above zero). It was experimentally shown that U6p electrons not only participate effectively in the inner valence molecular orbital formation but also participate strongly (more than 1 U6p electron) in the formation of the filled outer valence molecular orbitals.

Key words: XPS, X_α-DVM, uranium oxide, uranyl group, outer valence (OVMO) and inner valence (IVMO) molecular orbitals

INTRODUCTION

X-ray photoelectron spectra from uranium trioxide in the binding energy range 0–50 eV exhibit a complicated structure [1–6]. While studying the X-ray photoelectron spectra from actinide materials in this binding energy range, the observed lines were found to be several eV wide, which was wider than some corresponding core lines [3–8]. For instance, the O1s (E_b = 531.4 eV) line in the spectrum from γ-UO_3 is 2.2 eV wide, while the corresponding O2s line (E_b ~ 23.4 eV) was found to be more than 4 eV wide and structured [5–8]. According to the uncertainty ratio $\Delta E \Delta\tau \sim h/2\pi$, where h – Plank's constant, the natural width of the level from which an electron was removed ΔE is inversely proportional to the lifetime $\Delta\tau$ of the formed ion ("hole"). Since the lifetime of the "hole" ($\Delta\tau$) decreases while the absolute energy of the atomic level increases, for atoms the XPS lines of low-energy levels must be narrower. One of the reasons of the observed widening of the low-energy (0–50 eV) spectral lines of uranium trioxide is formation of the outer valence (OVMO) and inner valence (IVMO) molecular orbitals [3–8]. Practically, these spectra reflect the zone structure and appear as several eV wide bands. The IVMOs in uranium trioxide form due to strong overlapping of the U6p and O2s atomic shells of the neighboring atoms. Such strong overlapping of the U6p and O2s atomic orbitals (AO) was theoretically shown for uranyl group [4, 5, 9–13] and for the first time experimentally established on the basis of the XPS spectral structure parameters using the binding energy difference between the outer and core electron shells for uranium oxides γ-UO_3 and UO_2 [3–6], as well as for some other actinide (Th, U, Np, Pu, Am) compounds [7, 8]. That enabled identification of high-resolution conversion electron [14–16] and X-ray $O_{4,5}$(U) emission [17] spec-

Scientific paper
UDC: 539.194/.196:546.791
BIBLID: 1451-3994, *17* (2002), 1–2, pp. 3–12

Authors' addresses:
[1]Russian Research Center "Kurchatov Institute",
1, Kurchatov sq., Moscow 123182, Russia
[2]Institute of Solid-State Chemistry of Ural Dept. of RAS,
Ekaterinburg, Russia

E-mail address of corresponding author:
teterin@ignph.kiae.ru (Y. A. Teterin)

tra from uranium dioxide and trioxide. As a result, additional experimental evidence was obtained of the inner valence molecular orbital formation in uranium oxides.

Another important phenomenon we have experimentally observed recently is the effective participation of the filled valence An5f atomic shells in OVMO formation. Earlier, the An5f electrons were traditionally suggested to be promoted to, for instance, the An6d atomic orbitals before chemical bonds were established. Calculation results show that the An5f atomic shells can participate directly in the MO formation in actinide compounds [10, 11, 18]. This principally important fact needs experimental confirmation. The comparability of the experimental and theoretical partial An5f and An6p electron densities can serve as a criterion of correctness of the electronic structure calculation for actinide compounds.

The present work analyses the fine structure of the low-energy X-ray photoelectron, the conversion electron spectra of uranium trioxide taking into account the non-relativistic (NR X_α-DVM) and relativistic (R X_α-DVM) X_α Discrete Variation calculation results for the $[UO_2O_4]^{6-}$ cluster of D_{4h} symmetry group which reflects the uranium close environment in γ-UO_3.

EXPERIMENTAL

XPS spectra of solid-state uranium trioxide γ-UO_3 were taken with an HP-5950A spectrometer that uses monochromatized Al $K_{\alpha 1,2}$ ($h\nu$ = 1486.6 eV) X-rays utilizing a low energy electron flood gun for charge compensation under ~$1.3 \cdot 10^{-7}$ Pa at room temperature. Overall resolution measured as the $Au4f_{7/2}$ electron line full width half maximum (FWHM) was 0.8 eV. Electron binding energies (E_b) are given relative to the E_b of the C1s electrons from adventitious hydrocarbons at the sample surface defined as 285.0 eV. On the golden substrate E_b(C1s)=284.7 eV at E_b($Au4f_{7/2}$)=83.8 eV [7, 8]. The O1s spectrum from uranium trioxide was observed as a widened (Γ = 2.2 eV) asymmetric single line, while the C1s line was 1.3 eV wide. The measurement errors of line position and widths were ±0.1 eV, whereas relative line intensity errors were about 10%.

The γ-UO_3 sample for XPS measurements was prepared by pressing powder ground in the agate mortar into indium on the metallic substrate as a thick layer with a flat surface. This sample was used as an initial substrate for the implantation of the uranium isomer by electrostatic collection in oxygen atmosphere of recoiled ^{235m}U atoms yielded from ^{239}Pu α-decay for the conversion spectra measurements with the same spectrometer using additional accelerating electronic system [15, 16]. Calibration of the conversion electron spectra was done by XPS data for γ-UO_3. The XPS spectral background due to the inelastically scattered electrons was subtracted by Shirley [19]. For the conversion electron spectra it was subtracted by both Shirley and exponent [16]. Maximum relative intensity difference did not exceed 2%. Figure 1 shows the conversion electron spectrum with exponentially subtracted background.

The $[UO_2O_4]^{6-}$ (D_{4h}) cluster [20] reflecting uranium close environment in γ-UO_3 is represented by an uranyl ion surrounded by four more distant oxygen (ligand L) ions in the equatorial plane. The interatomic distances used in the calculations were $R_{U\text{-}O} = 1.79 \cdot 10^{-10}$ m and $R_{U\text{-}L(O)} = 2.30 \cdot 10^{-10}$m (Table 1). Relativistic X_α Discrete Variation method [21, 22] is based on the solutions of the Dirack-Slater equation for 4-component spinors that are linear combinations of atomic orbitals from solution of the relativistic equation for isolated atoms. The expanded basis of the numerical AOs was used in this work. U7p states were used beside the filled orbitals. The direct basis for the MO decomposition were symmetrized atomic orbitals

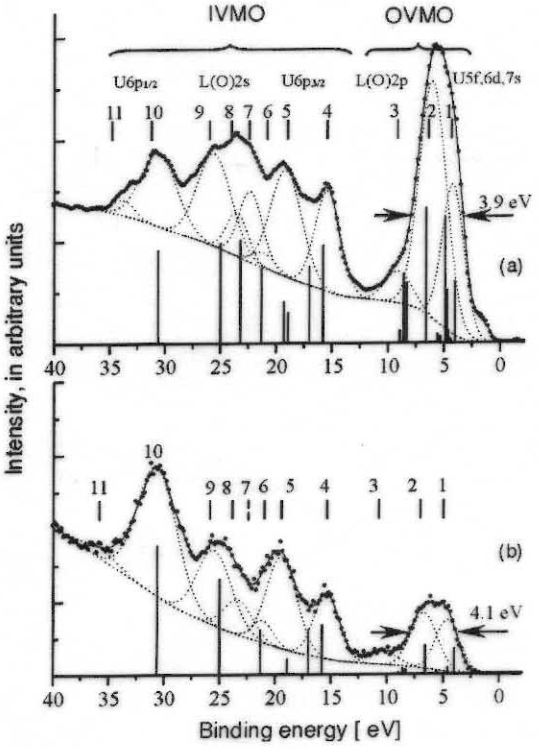

Figure 1. X-ray photoelectron (a) and conversion electron (b) spectra from γ-UO_3. The corresponding theoretical spectra (RX_α-DVM) are given under the experimental spectra as vertical lines. The shapes of the subtracted background and artificial subdivision of the spectra into separate components (1–11) are given as dashed lines. The spectral intensities are given in arbitrary units

(linear combinations of atomic orbitals) transformed by irreducible representations of the double D_{4h} groups [23]. Numerical integration for the determination of the matrix elements of the secular equation was done by the number of 4500 points in the cluster space to provide the convergence of the MO energies of not worse than 0.1 eV [24]. The local exchange-correlation potential was used in the form of X_α with α equal to the mean atomic value. Since the clusters are crystal fragments, the renormalization of occupancy of the filled valence AO ligands was used in the process of self-consistence. This enabled effective accounting of the stoichiometry of the compounds and charge redistribution between ligands and neighboring crystal [24]. For the correct estimation of the joint influence of the relativistic effects in uranium trioxide, the non-relativistic X_α–DVM calculation of the cluster with similar crystallographic and calculation parameters was taken into account [25].

RESULTS AND DISCUSSION

X-ray photoelectron spectrum of low-energy electrons (0–40 eV E_b) from γ-UO_3 can be conditionally subdivided into the two regions (Fig. 1). The first one 0–13 eV exhibits the structure deriving from electrons of the outer valence MOs formed mostly of the incompletely filled outer valence U5f,6d,7s and O2p AOs from the neighboring atoms (Table 1). The second one 13–40 eV consists of the structure originating from IVMOs formed mostly due to the strong interaction of the filled U6p and O2s AOs of the closest atoms. Since the parameters of such a structure correlate strongly with the interatomic distances of uranium-oxygen in the axial and equatorial directions in uranyl compounds, they have become the reason to subdivide the considered spectrum into the OVMO and IVMO [7, 26]. The OVMO spectral structure has three typical features and can be subdivided into three components. The IVMO region exhibits eight manifested peaks; therefore this region can be subdivided into eight components (Fig. 1). Despite the obvious formalism of such a subdivision, it allows qualitative and quantitative comparison of XPS parameters with the corresponding conversion of spectral parameters and theoretical calculation results for the $[UO_2O_4]^{6-}(D_{4h})$ cluster.

The results of the relativistic calculations for such a cluster and the MO composition are given in Table 1. Since after photoemission atoms transit into excited states with holes in certain levels, the electron binding energies calculated for the transition states should be used for a stricter comparison of theoretical and experimental results [27]. However, rough approximation suggests that the valence electron binding energies calculated for the transition state differ from those for ground state by a constant shift towards higher absolute energy. Therefore, the calculated MO energies were increased by 2 eV for the sake of comparison with the experimental binding energies (Table 2). The theoretical intensities of several spectral regions were determined by taking into account the MO composition (Table 1) and the photoemission cross-sections [28] (Table 2, Fig. 1). Comparing experimental spectra and theoretical data, the fact that X-ray photoelectron spectrum from uranium trioxide reflects the zone structure and consists of bands widened due to the solid-state effects has to be taken into account. Despite the calculation approximations, the qualitative agreement between the theoretical and experimental data was found. Indeed, the corresponding theoretical and total experimental widths and relative intensities of the outer and inner valence zones are comparable. Satisfactory agreement between the experimental and calculated, in particular, the U6s binding energies was established (Table 2). The worst discrepancy was found for the middle IVMO spectral region [$11\gamma_7^-(5)$–$10\gamma_7^-(8)$]. Earlier the non-relativistic results in the X_α approximation were used for interpretation of the X-ray photoelectron IVMO spectral structure [5, 25]. That allowed qualitative identification of the fine XPS spectral structure of uranium trioxide in the binding energy range 0–23 eV. That was possible because if taking into account the relativistic effects, the strong detaching of the $U6p_{1/2}$ component took place while the basic features of the structure in the range 0–23 eV remained permanent. Taking into account the relativistic effects in this work allowed practically the qualitative identification of such X-ray photoelectron spectrum in the whole range 0–40 eV.

Thus, the outer valence electron band intensity was found to arise due to the U5f,6d and O2p AO electrons and, to a great extent, to the U6p inner valence AO electrons of the close atoms. Practically, for the first time the experimental evidence for the direct participation of the U5f electrons in the chemical binding almost without loosing their f-nature was obtained. Indeed, the experimental intensity ratio OVMO/IVMO was found to be $I_{exp.} = 0.70$, which was comparable with the corresponding theoretical ratio $I_{theor.} = 0.93$ (Table 2). Since the U5f AOs practically do not participate in the IVMO formation, this difference may be explained by the decreasing of the photoemission cross-section of the U5f electrons participating in the chemical binding. However, suggestion that the OVMO band intensity comes up only from the $U6d^47s^2$ and $3O2p^4$ electrons and the IVMO – from the $U6p^6$ and $3O2s^2$ ones in uranium trioxide gives the corresponding theoretical ratio $I_{theor.} = 0.30$, which is significantly less than the observed experimental

Table 1. Composition (portion) and energies E_0 [eV] of MOs for the $[(UO_2)O_4]^{6-}(D_{4h})$ cluster at $R_{U\text{-}O} = 1.79\cdot10^{-10}$ m and $R_{U\text{-}L} = 2.30\cdot10^{-10}$ m (RX_α-DVM), photoemission cross-sections σ_i[a], and probabilities of inner conversion α_i[b]

MO		E_0	MO Composition												
			U									O		O_t	
		[eV]	6s	$6p_{1/2}$	$6p_{3/2}$	$6d_{3/2}$	$6d_{5/2}$	7s	$5f_{5/2}$	$5f_{7/2}$	$7p_{1/2}$	$7p_{3/2}$	2s	2p	2s	2p
			σ_i[a] 1.14 α_i[b] 0.10	0.89 61.2	1.29 26.9	0.61 5.55	0.55 6.09	0.12 0.01	3.67 0.10	3.48 0.05			0.96	0.07	0.96	0.07
OVMO	$24\gamma_6^+$	−13.4				0.40	0.60									
	$18\gamma_7^+$	−8.8				0.35	0.65									
	$17\gamma_7^+$	−6.5				0.20	0.80									
	$23\gamma_6^+$	−6.3				0.60	0.40									
	$27\gamma_6^-$	−5.7							0.16	0.08		0.76				
	$22\gamma_6^+$	−5.5						1.00								
	$26\gamma_6^-$	−4.8			0.08				0.13	0.33	0.45					
	$16\gamma_7^+$	−4.6				0.53	0.47									
	$25\gamma_6^-$	−4.4										1.00				
	$20\gamma_7^-$	−4.3										1.00				
	$19\gamma_7^-$	−1.7							0.16	0.75				0.05		0.04
	$24\gamma_6^-$	−1.6							0.30	0.58				0.04		0.08
	$23\gamma_6^-$	−1.3							0.27	0.63				0.03		0.05
	$18\gamma_7^-$	−1.1							0.30	0.58				0.01		0.10
	$17\gamma_7^-$	−0.6							0.53	0.32						0.14
	$16\gamma_7^-$	0.1							0.74	0.23						0.03
	$22\gamma_6^{-c}$	2.0			0.14				0.05					0.03		0.76
	$21\gamma_6^+$	2.0														1.00
	$15\gamma_7^-$	2.0			0.12									0.01		0.81
	$15\gamma_7^+$	2.4												0.07		0.91
	$20\gamma_6^+$	2.4												0.07		0.92
	$21\gamma_6^-$	2.6		0.03					0.02							0.92
	$14\gamma_7^-$	2.7							0.06	0.07						0.86
	$20\gamma_6^-$	2.9								0.13						0.84
	$13\gamma_7^-$	2.9							0.18							0.78
	$19\gamma_6^+$	3.3	0.04					0.02								0.90
	$14\gamma_7^+$	3.5					0.09									0.91
	$13\gamma_7^+$	3.6				0.09	0.02									0.90
	$19\gamma_6^-$	4.6		0.05	0.18				0.09	0.17				0.32		0.18
	$12\gamma_7^-$	6.3			0.05				0.04	0.08				0.80		0.03
	$18\gamma_6^+$	6.6	0.07				0.04						0.04	0.81		0.02
	$18\gamma_6^-$	6.6		0.02					0.09	0.03				0.84		
	$12\gamma_7^+$	6.9				0.02	0.05							0.89		0.04
	$17\gamma_6^+$	7.0				0.06	0.02							0.88		0.04
IVMO	$17\gamma_6^-$	13.8		0.01	0.48								0.24	0.21	0.05	0.01
	$11\gamma_7^-$	15.0			0.46									0.04	0.49	0.01
	$16\gamma_6^-$	16.9		0.07									0.05		0.86	
	$16\gamma_6^+$	17.3													0.97	0.01
	$11\gamma_7^+$	17.3													0.98	
	$10\gamma_7^-$	19.3			0.45										0.49	0.04
	$15\gamma_6^+$	21.2	0.07										0.89			
	$15\gamma_6^-$	23.0		0.32	0.24								0.31	0.03	0.07	0.02
	$14\gamma_6^-$	28.6		0.56	0.04								0.30	0.09		
	$14\gamma_6^+$	44.1	0.93										0.03	0.03		

a) photoionization cross-sections σ_i [in 10^{-25} m² per one electron] from the work [28]
b) relative partial conversion probabilities α_i [%] for E3-multipole of ^{235}U nucleus with participation of the electrons from the nlj-shells obtained on the basis of the work [34]
c) upper filled molecular orbital (2 electrons), filling number for all orbitals is 2

ratio [29]. This contradicts the traditional in chemistry suggestion that the U5f electrons before participation in the chemical binding have to be promoted to the U6d shell. Therefore, the relativistic calculation results can be suggested to reflect correctly the U5f partial electronic density (Table 2). These data show that about two U5f electrons participate directly in the chemical binding, while the vacant U5f electronic states lie in the range of 6 eV around the absorption edge (Table 1). This agrees qualitatively with the data of the X-ray $O_{4,5}(U)$ emission spectroscopy [17] and the near edge $O_{4,5}(U)$ absorption spectroscopy for uranium trioxide [30].

In the IVMO spectral range the best agreement was found only for the $17\gamma_6^-(4)$, $15\gamma_6^-(9)$, and $14\gamma_6^-(10)$ IVMO characterizing the total spectral width. Despite the comparability of the theoretical and experimental summary relative intensities, the calculated $11\gamma_7^-(5)$–$10\gamma_7^-(8)$ IVMO energies differ significantly from the corresponding experimental values (Table 2).

Taking into account the non-relativistic data for uranyl group $[UO_2]^{2+}(D_{\infty h})$ and the $[UO_2O_4]^{6-}$ (D4h) cluster [25], the experimental binding energy

Table 2. Parameters of X-ray photoelectron and conversion electron spectra from UO_3 and results of calculations for the $[(UO_2)O_4]^{6-}(D_{4h})$ cluster at $R_{U\text{-}O} = 1.79 \cdot 10^{-10}$ m and $R_{U\text{-}L} = 2.30 \cdot 10^{-10}$ m (relativistic X_α - DVM), and the U6p-state density ρ_i (e^-)

	MO	$-E$ [eV]	X-ray photoelectron spectrum			Conversion electron spectrum			Experimental density ρ_i of the U6p states in e^- units	
			Energy[c] [eV]	Intensity [%]		Energy[c] [eV]	Intensity [%]			
			Experiment	Theory	Experiment	Experiment	Theory	Experiment	$U6p_{3/2}$	$U6p_{1/2}$
OVMO	$22\gamma_6^{-}$[a]	4.0		3.5			3.0			
	$21\gamma_6^{+}$	4.0		0.1						
	$15\gamma_7^{-}$	4.0		1.5			2.6			
	$15\gamma_7^{+}$	4.4		0.2						
	$20\gamma_6^{+}$	4.4		0.2						
	$21\gamma_6^{-}$	4.6		1.0			1.5			
	$14\gamma_7^{-}$	4.7	4.2 (2.3)	4.4	12.8	4.6 (2.5)		7.3		
	$20\gamma_6^{-}$	4.9		4.3						
	$13\gamma_7^{-}$	4.9		6.2						
	$19\gamma_6^{+}$	5.3		0.6						
	$14\gamma_7^{+}$	5.5		0.6			0.4			
	$13\gamma_7^{+}$	5.6		0.7			0.5			
	$19\gamma_6^{-}$	6.6	6.0 (2.9)	11.3	25.2	6.7 (2.8)	6.3	8.6		
	$12\gamma_7^{-}$	8.3		5.2			1.1			
	$18\gamma_6^{+}$	8.6		1.8			0.2			
	$18\gamma_6^{-}$	8.6		4.7			1.0			
	$12\gamma_7^{+}$	8.9		1.0			0.3			
	$17\gamma_6^{+}$	9.0	9.0 (2.8)	1.0	3.3	10.4 (3.0)	0.4	2.3		
	ΣI_i[b]			48.3	41.3		17.3	18.2	0.2	1.1
IVMO	$17\gamma_6^{-}$	15.8	15.4 (2.7)	8.1	10.0	15.4 (2.7)	10.7	9.7		0.8
	$11\gamma_7^{-}$	17.0	19.1 (3.3)	6.4	13.1	19.4 (3.2)	9.8	16.1		1.4
	$16\gamma_6^{-}$	18.9	21.1 (2.5)	2.6	1.4	21.1 (2.2)	3.4	2.7	0.1	
	$16\gamma_6^{+}$	19.3	22.3 (2.5)	1.7	6.6					
	$11\gamma_7^{+}$	19.3		1.7						
	$10\gamma_7^{-}$	21.3	23.5 (2.3)	6.3	3.7	23.3 (3.0)	9.6	5.8		0.5
	$15\gamma_6^{+}$	23.2		8.7						
	$15\gamma_6^{-}$	25.0	25.6 (3.6)	8.4	12.3	25.5 (3.7)	20.8	15.3	0.5	0.2
	$14\gamma_6^{-}$	30.6	30.6 (3.8)	7.8	10.4	30.6 (4.2)	28.3	30.2	1.1	
	Sat		33.7 (2.2)		1.2	35.6 (3.5)		2.0	0.1	
	ΣI_i[b]			51.7	58.7		82.7	81.8	1.8	2.9
	$14\gamma_6^{+}$	46.1	47.0 (6.1)							

a) upper filled molecular orbital (2 electrons), filling number for all orbitals is 2
b) summary densities of the U6p – electronic states and line intensities
c) line widths given in parenthesis in [eV]

differences between the outer and core electron levels of uranium [31], as well as uranium trioxide (see for example [7, 26, 32]) in the MO LCAO (molecular orbitals as linear combinations of atomic orbitals) approximation the MO schematic can be built (Fig. 2). This schematic allows understanding of the real structure of the X-ray photoelectron spectrum from uranium trioxide. This approximation allows conditional distinguishing of the $17\gamma_6^{-}(4)$, $15\gamma_6^{-}(9)$ and $14\gamma_6^{-}(10)$ IVMOs characterizing the binding and interatomic distance in uranyl group UO_2^{2+}, and the $11_7^{-}(5)$ and $10\gamma_7^{-}(8)$ IVMOs characterizing the binding and interatomic distance in the equatorial plane of the considered cluster, as well as the quasiatomic $16\gamma_6^{-}(6)$, $16\gamma_6^{+}(7)$, $11\gamma_7^{+}(7)$ and $15\gamma_6^{+}(7)$ IVMOs due to the O(L)2s AOs of oxygen of two kinds (O and L). It has to be noted that such subdivision into the IVMOs is experimentally grounded [7, 26, 32]. These experimental data show that energies of the quasiatomic $16\gamma_6^{-}(6)$–$-15\gamma_6^{+}(7)$ IVMOs should be close by the magnitude. Indeed, as it follows from the O1s spectrum of γ-UO_3, their chemical nonequivalence should not exceed 0.9 eV, since this line was observed asymmetric 2.2 eV wide, while the binding energy should be about 23.4 eV since $\Delta E_{L,O} = 508$ eV and the O1s binding energy in γ-UO_3 is $E_b = 531.4$ eV (Fig. 2). Taking into account that $\Delta E_U = 360.6$ eV, $\Delta E_1 = 363.0$ eV, the values $\Delta_2 = 2.4$ eV and $\Delta_1 = 3.7$ eV [7, 26, 32] can be found. Since the energy difference of the $14\gamma_6^{-}(10)$ and $17\gamma_6^{-}(4)$ IVMOs is 15.2 eV, and the U6p spin-orbit splitting in an atom according to calculation [33] and experimental [31] data is $\Delta E_{so}(U6p) = 10.0$ eV, the perturbation $\Delta_3 = 2.6$ eV can be evaluated and compared with $\Delta_2 = 2.4$ eV. On the basis of these data it follows that the contribution of U6p AOs in $11\gamma_7^{-}(5)$ and $14\gamma_6^{-}(10)$ must be significantly bigger, while in the $10\gamma_7^{-}(8)$ it is significantly smaller than in $17\gamma_6^{-}(4)$ IVMO. Line widths of the quasiatomic $16\gamma_6^{-}(6)$–$15\ \gamma_6^{+}(7)$, as expected, are smaller than those of other IVMOs. The observed relative narrowing of the $17\gamma_6^{-}(4)$ IVMO line can be explained by partial loss of the antibonding nature of this MO due to the significant admixture (21%) of O2p AO (Table 2, see also ref. [8]).

One of experimental confirmations of IVMO formation in uranium trioxide is its high-resolution

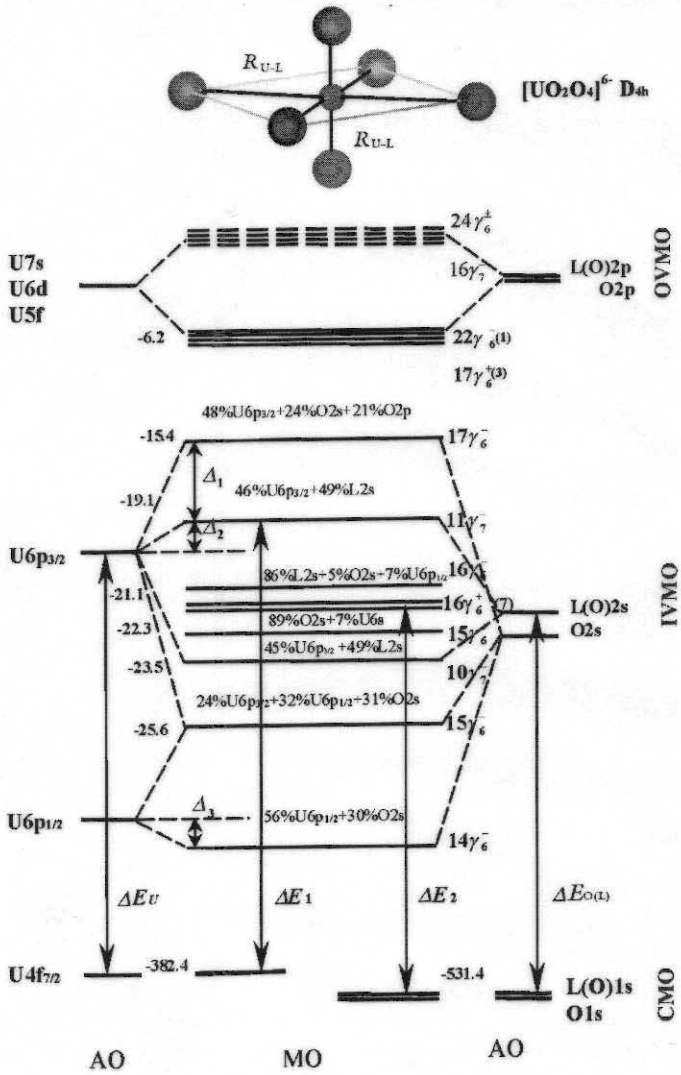

Figure 2. Diagram of MO in the $[UO_2O_4]^{6-}(D_{4h})$ cluster built taking into account theoretical and experimental data. Chemical shifts at the cluster formation are not shown. Some energy differences measurable experimentally are presented as arrows. Experimental XPS binding energies in eV are given at the left. Energetic scale is not kept

conversion electron spectrum measured for the first time in [14, 15]. Identification of the structure of this spectrum was done on the basis of the XPS parameters of this compound using the OVMO and IVMO conceptions [3–8]. This spectrum was measured tens of times by using different techniques of sample preparation in our Laboratory [16], and its interpretation made it obvious that such spectra could serve as a quantitative measure of the correctness of the theoretical calculations for uranium trioxide (Fig. 1).

The fully converted transition of E3 multipole of ^{235m}U ($T_{1/2}$ = 26.3 ± 0.2 min for UO_3) isomer nuclei from the first excited state (spin $I_1 = 1/2^+$, $E_1 = 76.5 \pm 0.4$ eV) to the ground nuclei state (spin $I_0 = 7/2^-$, $E_0 = 0$ eV) is accompanied by the emission of low-energy electrons. The conversion is energetically allowed for the $U6s^26p^65f^36d^17s^2$ electrons whose shells can participate effectively in OVMO and IVMO formation in uranium compounds. In this case the partial conversion probabilities with the yield of the $(n_il_ij_i)$ electron to the continuous spectrum with kinetic energy $\varepsilon_i\, \alpha_i(EL, I_1 \to I_0, n_il_ij_i \to \varepsilon_i)$, normalized per one electron, where n_i – main quantum number, l_i – and j_i – orbital and full angular moments of the electron, are proportional to electronic factors $w_\lambda(E3, n_il_ij_i, \hbar\omega)$, where $\hbar\omega$ – energy of the excited nucleus [34].

In this work the corresponding theoretical spectrum was obtained by using the results of relativistic calculation for γ-UO_3 and the relative one-electron conversion cross-sections for comparison with the experimental conversion spectrum (Fig. 1). From the relative one-electron conversion cross-sections (Table 2) obtained on the basis of the data of [34] it follows that the conversion spectrum of uranium trioxide practically reflects partial U6p

electronic state density. The cross-section for $U6p_{1/2}$ electrons is about 2.3 times higher than the corresponding cross-section for $U6p_{3/2}$ electrons. With this in mind, the observed satisfactory agreement between the experimental X-ray photoelectron and conversion spectra (Fig. 1) has to be noted. Despite the fact that errors can arise both from the use of the results for the ground state in determination of the conversion electron spectral line intensities and from the background subtraction [16], the qualitative agreement between the theoretical and experimental conversion spectra was observed. Comparison of X-ray photoelectron and conversion electron spectra leads to three important conclusions. The first one – U6p shell participates effectively in IVMO formation. The second – U6p shell participates strongly also in OVMO formation. The third – electrons of oxygen quasiatomic $16\gamma_6^+(7)$, $11\gamma_7^+(7)$, and $15\gamma_6^+(7)$ orbitals, as expected, were practically not observed in the conversion spectrum at 23.4 eV, and $11\gamma_7^-(5)$, $16\gamma_6^-(6)$, $10\gamma_7^-(8)$ IVMO energies differ significantly from the corresponding theoretical energies and mostly agree with the experimental XPS values (Fig. 1, 2).

For the purpose of comparative qualitative analysis of the experimental and theoretical line intensities the considered spectra were divided on the ground of the data in the diagram (Fig. 2). The binding energies were taken from the experiment (Fig. 3), and the theoretical intensities – from the calculations (Table 2). The results of identification of the XPS and conversion electron spectral structures are given in Table 2 and Fig. 3. These data show that the experimental binding energies of the X-ray photoelectron and conversion spectra practically coincide. However, the experimental IVMO intensities in many cases differ significantly from the corresponding theoretical results. The best coincidence was observed for the $17\gamma_6^-(4)$, $16\gamma_6^-(6)$, and $14\gamma_6^-(10)$ IVMO lines. Taking into account the conversion cross-sections and the conversion spectral line intensities, the $U6p_{3/2,1/2}$ partial electronic density for uranium trioxide was evaluated (Table 2). It was found that 1.3 U6p electrons participate in the OVMO formation, which is comparable with the corresponding theoretical value 1.0 (Table 1). In the OVMO formation the main part is taken by $U6p_{3/2}$ electrons. For the IVMO energy region in some cases an agreement was observed. For example, the antibonding $17\gamma_6^-(4)$ IVMO consists of 0.8 $U6p_{3/2}$ electrons, which is comparable to the corresponding calculated result (0.98 e^-, Table 1). A similar agreement was observed for $14\gamma_6^-(10)$ IVMO bonding. From the data for the antibonding $11\gamma_7^-(5)$ and the corresponding bonding $10\gamma_7^-(8)$ IVMO it is evident that the calculated U6p and O2s AO overlapping is about twice as high as the corresponding experimental value.

Since from the quantum mechanics on the qualitative level it is known how the line intensities of the considered spectra must change with the changing of the level energies, we can consider ways how to arrive at an agreement between the experimental and theoretical results. As it was shown in [7, 8, 26], the wider the MO lines are, the more active parts (bonding, antibonding) the AOs take in formation of the MOs. The narrowest observed lines were the ones deriving from the nonbonding or quasiatomic MOs. Therefore, the $17\gamma_6^-(4)$ IVMO line is narrow because of the relatively high O2p contents in it. It also leads to the noticeable decrease of its intensity and losing of its antibonding nature (Figs. 2, 3). The observed discrepancy in the considered $11\gamma_7^-(5)$ IVMO intensities confirms the suggestion that the participation of U6p AO in it has to be about twice higher than in formation of $17\gamma_6^-(4)$ IVMO (Table 2). U6p AO plays approximately the same part in the corresponding binding $10\gamma_7^-(8)$ IVMO. Unfortunately, it is difficult to establish the reliably of $10\gamma_7^-(8)$ IVMO line width. But from the data of the conversion electron spectra

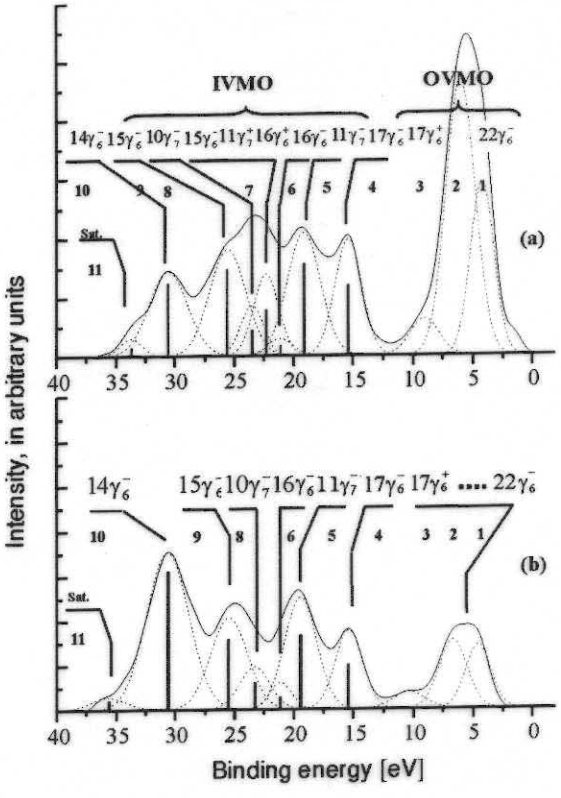

Figure 3. X-ray photoelectron (a) and conversion electron (b) spectra from γ-UO_3 with subtracted background. Corresponding spectra calculated by means of theoretical and experimental data are presented under the experimental spectra as vertical lines for comparison. The spectral intensity is given in arbitrary units

(Table 2) it follows that the antibonding nature of the $11\gamma_7^-(5)$ IVMO is comparable with the bonding nature of the $10\gamma_7^-(8)$ IVMO. In other words, the electrons of this IVMO couple must bring zero contribution into the covalent component of the chemical bond in UO_3.

The most ambiguous for the interpretation remains the $16\gamma_6^-(6)$–$10\gamma_7^-(8)$ IVMO energy range. The comparison of the X-ray photoelectron and conversion electron spectra shows that the structure of this range mostly results from O(L)2s electrons, which agrees with the calculation data. However, in the calculations the influence of the U6p–L2s-equatorial oxygen AO overlapping during the $11\gamma_7^-(5)$ and $10\gamma_7^-(8)$ IVMO formation was overestimated. This led to the violation of the sequence order $16\gamma_6^-(6)$–$10\gamma_7^-(8)$ IVMO. This can be due to the fact that the interatomic distances in the equatorial planes of the cluster $[(UO_2)O_4]^{6-}(D_{4h})$ used in the calculations were set too low in comparison with the real distances. With this in mind, in this work this spectral region was decomposed. The knowledge of the correct IVMO sequence is especially important for the evaluation of the contribution of the IVMO electrons in the covalent component of the chemical bond in UO_3. The observed peaks (11) in the considered spectra can be attributed, in particular, to the shake-up process accompanying the electron photoemission.

In conclusion, we will note that despite some approximations used for calculation of the electronic structure of the $[UO_2O_4]^{6-}$ (D_{4h}) cluster that reflects the uranium close environment in γ-UO_3, the obtained results agree qualitatively with the experimental data, which allowed reliable identification of the lines attributed at least to the upper IVMO electrons. This allows usage of these data, in particular, in the determination of the structure and interatomic distances in uranyl compounds [7, 26, 32], as well as for the interpretation of the structures of various X-ray spectra from uranium materials.

CONCLUSION

Low-energy X-ray photoelectron and conversion electron spectra from uranium trioxide were measured, and calculations were done for $[UO_2O_4]^{6-}(D_{4h})$ cluster that reflects the structure of uranium close environment in γ-UO_3 in the non-relativistic and relativistic X_α-DVM approximation. This enabled a satisfactory qualitative and in some cases quantitative agreement between the experimental and theoretical data, and interpretation of such spectra.

1. Despite the traditional opinion that before participation in chemical binding the U5f electrons could be promoted to the higher (for example – U6d) levels, the U5f electrons (about two U5f electrons) theoretically proved and experimentally confirmed to be able to participate directly in the chemical bond formation in uranium trioxide. The filled U5f states were shown to be localized in the outer valence MO binding energy range 4–9 eV, while the vacant U5f states – generally localized in the low-energy range (0–6 eV above zero).

2. It was experimentally shown that U6p electrons not only participate effectively in the inner valence MO formation, but also strongly participate (more than 1 U6p electron) in the formation of the filled outer valence MOs. This agrees with the calculation data.

3. The results of the relativistic calculations confirmed that the inner valence MO system formed mostly of the U6p and O(L)2s atomic orbitals of uranium and ligands could be divided into two MO groups, one of which – $17\gamma_6^-(4)$, $15\gamma_6^-(9)$, $14\gamma_6^-(10)$ – characterizes the bond in the axial direction, and the other one – $11\gamma_7^-(5)$, $10\gamma_7^-(8)$ – in the equatorial plane. This is important in connection with the development of the experimental technique for the determination of the interatomic distances in the axial direction and equatorial plane of uranium oxides and other oxygen-containing uranium compounds on the basis of the experimental X-ray photoelectron spectra of electrons from the inner valence molecular orbitals.

ACKNOWLEDGEMENT

The present work was supported by the RFBR (grant No. 00-03-32138a) and ISTC (grant No. 1358).

REFERENCES

[1] Verbist, J., Riga, J., Pireaux, J. J., Caudano, R., X-Ray Photoelectron Spectra of Uranium and Uranium Oxides. Correlation with the Half-Life of $^{235}U^m$, *J. Electron Spectroscopy Related Phenomena, 5* (1974), pp. 193–205

[2] Veal, B. W., Lam, D. J., Carnall, W. T., Hoekstra, H. R., X-Ray Photoelectron Spectroscopy Study of Hexavalent Uranium Compounds, *Phys. Rev. B., 12* (1975), pp. 5651–5663

[3] Teterin, Yu. A., Kulakov, V. M., Baev, A. S., Zelenkov, A. G., Melnikov, I. A., Nevzorov, N. B., Streltsov, V. A., Determination of the Oxidation Degree of the Uranium Ions in Natural Uranium Oxides by XPS Method (in Russian), Book of abstracts, All-Union Conference "X-ray and X-ray photoelectron spectra and electronic structure of metals, alloys and compounds", Physical-Technical Institute, Izhevsk: Russia, 1979, p. 25

[4] Teterin, Yu. A., Baev, A. S., Vedrinsky, R. V., Gubsky, A. L., Zelenkov, A. G., Kovtun, A. P., Kulakov, V. M., Sachenko, V. P., Display of the Hybridization of the inner U6p-, O2s-orbitals of UO_2 and γ-UO_3 Oxides in the X-ray Photoelectron spectra (in Rus-

sian), in: Physical and mathematical methods in coordination chemistry, Shtiintsa, Kishinev, USSR, 1980, pp. 76–77

[5] Teterin, Yu. A., Baev, A. S., Vedrinsky, R. V., Gubsky, A. L., Zelenkov, A. G., Kovtun, A. P., Kulakov, V. M., Sachenko, V. P., XPS Spectral Structure of the Lowenergy Electrons of the UO_2 and γ-UO_3 Oxides, (in Russian), Doklady Akademii Nauk SSSR, *256* (1981), 2, pp. 381–384

[6] Teterin, Yu. A., Kulakov, V. M., Baev, A. S., Nevzorov, N. B., Melnikov, I. V., Streltsov, V. A., Mashirov, L. G., Suglobov, D. N., Zelenkov, A. G., A Study of Synthetic and Natural uranium Oxides by X-ray Photoelectron Spectroscopy, *Phys. Chem. Minerals., 7* (1981), pp. 151–158

[7] Teterin, Yu. A., Baev. A. S., X-ray photoelectron spectroscopy of actinide compounds (in Russian), TsNII Atominform, Moscow, 1986, p. 102

[8] Teterin, Yu. A., Gagarin, S. G., Inner Valence Molecular Orbitals and the Structure of X-ray Photoelectron Spectra, *Russian Chemical Reviews, 65* (1996), 10, pp. 825–847

[9] Ellis, D. E., Rosen, A., Walch, P. F., Applications of the Dirac-Slater Model to Molecules, *Int. J. Quant. Chem. Symp., 9* (1975), pp. 351–358

[10] Walch, P. F., Ellis, D. E., Effects of Secondary Ligands on the Electron Structure of Uranyl, *J. Chem. Phys., 65* (1976), 6, pp. 2387–2392

[11] Boring, M., Wood, J. H., Moskowitz, J. W., Self-consistent Field Calculation of the Electronic Structure of the Uranyl Ion (UO_2^{2+}), *J. Chem. Phys., 63* (1975), 2, pp. 638–642

[12] Wood, J. H., Boring, M., Woodruff, S. B., Relativistic Electronic of UO_2^{++}, UO_2^{+} and UO_2, *J. Chem. Phys., 74* (1981), 9, pp. 5225–5233

[13] Glebov, V. A., Electronic structure and properties of uranyl compounds (in Russian), Energoatomizdat, Moscow, 1983, p. 88

[14] Zhudov, V. I., Zelenkov, A. G., Kulakov, V. M., Odinov, B. V., Teterin, Yu. A., Investigation of the Influence of a Chemical Environment on the Conversion Electron Spectrum of (1/2 +) uranium-235 isomer (in Russian), Book of abstracts, XXX All-Union conference "Nuclear spectroscopy and the nuclei structure", Nauka, Leningrad, Russia, 1980, p. 614

[15] Grechukhin, D. P., Zhudov, V. I., Zelenkov, A. G., Kulakov, V. M., Odinov, B. V., Soldatov, A. A., Teterin, Yu. A., Direct observation of the Strong Hybridization of the Electronic Orbits in Spectra of Electrons of the Internal Conversion (in Russian), *Sov. Tech. Phys. Lett., 31* (1980), 11, pp. 627–630

[16] Panov, A. D., Zhudov, V. I., Teterin, Yu. A., Conversion Spectra of the Valence Shells Electrons of Uranium Compounds Containing Oxygen (in Russian), *Zhurnal Strukturnoi Khimii, 39* (1998), 6, pp. 1048–1051

[17] Teterin, Yu. A., Terekhov, V. A., Teterin, A. Yu., Ivanov, K. E., Utkin, I. O., Lebedev, A. M., Vukchevich, L., Inner Valence Molecular Orbitals and Structure of X-Ray $O_{4,5}$(Th,U) Emission Spectra in Thorium and Uranium Oxides, *J. Electr. Spectr. Relat. Phenom, 96* (1998), pp. 229–236

[18] Gubanov, V. A., Rosen, A., Ellis, D. E., Electronic Structure and Bonding in ThO_2 and UO_2, *Sol. St. Com., 22* (1997), 4, pp. 219–223

[19] Shirley, D. A., High-resolution X-Ray Photoemission Spectrum of the Valence Band of Gold, *Phys. Rev. B., 5* (1972), 12, pp. 4709–4714

[20] Mihailov, Yu. N., Crystal-chemistry of Coordination Compounds of Uranyl (in Russian), in: Problems of coordination chemistru, Chemistry of platinum and heavy elements, Nauka, Moscow, 1975, pp. 127–160

[21] Rosen, A. Ellis, D. E., Relativistic Molecular Calculations in the Dirac-Slater Model, *J. Chem. Phys., 62* (1975), 8, pp. 3039–3049

[22] Gubanov, V. A., Rosen, A., Ellis, D. E., Electronic Structure of Mono- and Dioxides of Thorium and Uranium, *J. Inorg. Nucl. Chem., 41* (1979), pp. 975–986

[23] Meyer, J., Sepp, W. D., Fricke, B., Computation on Relativistic Symmetry Orbitals for Finite Double Point Groups, *Computer Physics Communications, 54* (1989), pp. 55–73

[24] Ryzhkov, M. V., Gubanov, V. A., Teterin, Yu. A., Baev, A. S., Electronic Structure and X-Ray Photoelectron Spectra of Uranyl Compounds, *Radiohimiya, 1* (1991), pp. 22–28

[25] Teterin, Yu. A., Ryzhkov, M. V., Gubanov, V. A., Gagarin, S. G., The Role of Electron of the Low-Energy Filled Subshells of the Neighboring Atoms in Chemical Bond of Uranium Compounds, DAN SSSR, *284* (1985), 4, pp. 915–920

[26] Teterin, Yu. A., Baev, A. S., Ivanov, K. E., Mashirov, L. G., Suglobov, D. N., X-Ray Photoelectron Spectrum Structures of Low-Energy Electrons of uranium Compounds and Their Constructions (in Russian), *Radiokhimiya, 38* (1996), 5, pp. 395–402

[27] Slater, J. C., Johnson, K. H., Self-Consistent-Field Xα Cluster Method for Polyatomic Molecules and Solids, *Phys. Rev. B., 5* (1972), 3, pp. 844–853

[28] Band, I. M., Kharitonov, Yu. I., Trzhaskovskaya, M. B., Photoionization Cross Sections and Photoelectron Angular Distributions for X-Ray Line Energies in the Range 0.132-4.509 keV, Targets: $1 \leq Z \leq 100$, *Atomic Data and Nuclear Data Tables, 23* (1979), pp. 443–505

[29] Teterin, Yu. A., The An5f-states of Actinides (Th, U, Np, Pu, Am, Cm, Bk) in Compounds and Parameters of Their X-Ray Photoelectron Spectra (in Russian), *Kondensirovannye sredy i mezhfaznye granitsy, 2* (2000), 1, pp. 60–66

[30] Kalkowski, G., Kaindl, G., Brewer, W. D., Krone, W., Near-edge X-Ray-Absorption Fine Structure in Uranium Compounds, *Phys. Rev. B., 35* (1987), 6, pp. 2667–2677

[31] Fuggle, J. S., Burr, A. F., Watson, L. M., Fabian, D. Y., Lang, W., X-Ray Photoelectron Studies of Thorium and Uranium, *J. Phys. F: Metal. Phys., 4* (1974), 2, pp. 335–342

[32] Teterin, Yu. A., Ivanov, K. E., X-Ray Photoelectron Spectra Structure of Uranium Compounds Stipulated by Electrons of the Inner Valence Molecular Orbitals (IVMO), *Surface Investigation, 13* (1998), pp. 623–635

[33] Huang, K. N., Aojogi, M., Chen, M. N., Graseman, B., Mark, H., Neutral-atom Electron Binding Energies From Relaxed-Orbital Relativistic Hartree--Fock-Slater Calculations $2 \leq Z \leq 106$, *Atom. Data and Nucl. Data Tables, 18* (1976), pp. 243–291

[34] Grechukhin, D. P., Soldatov, A. A., Conversion E3-Transition From Isomer ^{235}U (73 eV) State (in Russian), *Nuclear Physics, 23* (1976), 2, pp. 273–281

Јурий А. Тетерин, Михаил В. Рижков, Антон Ј. Тетерин, Александер Д. Панов, Антон С. Никитин, Кирил Е. Иванов, Игор О. Уткин

ПРИРОДА ХЕМИЈСКИХ ВЕЗА У ТРИОКСИДУ γ-UO_3

Измерени су спектри фотоелектрона насталог дејством нискоенергетског X-зрачења као и конверзионог електрона у уранијумтриоксиду, и обављени су прорачуни $[UO_2O_4]^{6-}$ (D_{4h}) кластера који рефлектује непосреднију структуру уранијумске околине у γ-YO_3, у релативистичкој и нерелативистичкој X_α-DVM апроксимацији. Ово је омогућило задовољавајуће квалитативно, а у неким случајевима и квантитативно слагање експерименталних и теоријских података, као и интерпретацију ових спектара. Упркос традиционалном мишљењу да U5f електрони треба да запоседну више (на пример U6d) нивое пре учешћа у хемијским везама, показано је теоријски и потврђено експериментално да U5f електрони (око два U5f електрона) могу непосредно да партиципирају у образовању хемијских веза у уранијумтриоксиду. Показано је да су попуњена U5f стања локализована на спољашњим валентним молекуларним орбитама у енергетском опсегу од 4–9 eV, док су незапоседнута U5f стања начелно локализована у ниској енергетској зони (0–6 eV изнад нуле). Експериментално је потврђено да Uбр електрони не само да ефективно учествују у формирању унутрашњих валентних молекуларних орбита, већ такође јако партиципирају (више од једног Uбр електрона) у образовању попуњених спољашњих валентних молекуларних орбитала.